Physical and FEM Simulation of Microprobe Insertion into Rat Brain

A. E. Olamat, N. Nkemasong, B. M. Pohl and U. G. Hofmann
University of Lübeck, Institute for Signal Processing, Lübeck, Germany

hofmann@isip.uni-luebeck.de

Abstract: In order to investigate the implantation of microprobes into brain tissue, we developed a finite-element and a physical model to replace real biological tissue for mechanical testing. Penetrating forces of a tungsten indenter into a layered structure was investigated with different indentation speeds. Numerical and physical model are in good correspondence to each other and reproduce measured brain elasticity (15kPa) and dimpling effects followed by rupturing of the top layer well. We suggest for future mechanical evaluation of brain probes to first utilize model structures before sacrificing animals.

Keywords: microprobes, indentation, dimpling.

1. Introduction

One of the most exciting developments during the last few years connecting basic research with almost immediately useful clinical technology was the successful application of multiwire neuronal recordings with advanced signal processing to utilize intracortical neuronal signals to control devices [2-6]. Unfortunately penetrating rigid microelectrode arrays traumatize surrounding tissue in such a way, as to render the recording sites over time useless due to severe foreign-body reaction [7-12].
The first development of flexible microprobes [13] carrying microelectrodes (for recording and stimulation) in parallel with appropriate chemical surface coating [14] or even living cells [15, 16] holds the promise for an optimized integration into brain tissue.
Still, not too much attention has been given to the implantation procedure itself, besides the development of the pneumatic inserter for bed-of-nail type silicon arrays [17]. On the other hand, slow and gentler implantation of microprobes is known to cause a severe dimpling effect and as such may damage superficial neuropil even before the immune response starts.
In the following, we want to introduce a physical and computational small scale model of the brain surface as it is usually exposed by a craniotomy in laboratory animals. The purpose of our models is to test and improve the mechanical properties of new multisite microprobes during insertion without the need for animals.

2. Materials and Methods

2.1 Computational finite-element model

An axisymmetric indentation model of a layered structure was developed using COMSOL 3.5a (Comsol Multiphysics GmbH, Göttingen). The model had three components (see Fig. 1) - a flat tip cylindrical probe (the „microprobe“), one thin elastic layer (the „pia mater membrane“) and viscoelastic bulk material under it.

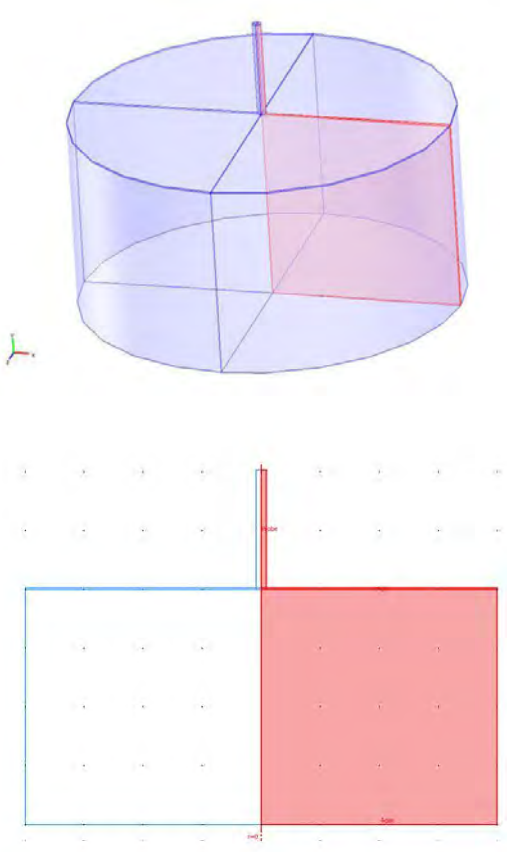

Figure 1: (top) 3D model of an indenter-membrane-bulk structure, (bottom) 2D view and half slice of the same model.

The „microprobe“ was simulated as a flat ended cylinder with 90µm diameter and 1mm in length. Its material properties were set to match Tungsten with a Young's modulus E=3.6x10^{11}Pa and Poisson's ratio v=0.27.
The „pial membrane“ was designed to match an elastic material formed of PE-polymer (E=2.9x10^{9}) and v=0.33 [18].
The bulk material is modeled by a generalized Maxwell model [19] with the associated model parameters of 1% (w/v) agar-gel shown in Table 1.

G (kPa)	G_i (kPa)	τ_i (s)
4.667	1.416	14.41
	4.977	159.62

Table 1: viscoelastic parameters of Agar material

Foil-layer which is located between the probe and the Agar has a 15µm of thickness and 4mm of diameter, the Agar which is the biggest object modeled as cylinder of 4mm of diameter and 2mm of height.

The microprobe was loaded with a predescribed displacement in z-direction with R_z=v*t (R_z: the displacement, v: velocity of the probe motion, t: elapsed-time of the probe motion). The probe was fixed in the r-direction at R_r=0; the left hand side boundary of all three parts complies to a symmetry plane condition; the right hand side of the membrane-layer is fixed, the right hand side and bottom of the bulk are fixed too, all other boundaries are left free.
We solved our model as an axisymetric problem with the COMSOL provided method as a transient analysis. The neccessary elapsed time parameter was deduced from the experimental indentation data.

2.2. Physical indentation model

A 1% (w/v) agar gel was prepared by dissolving microbiological grade granulated agar (Agarose NEEO, Carl Roth GmbH, Karlsruhe, Germany)) in distilled water. The solution was heated to boiling in an Erlenmeyer flask on a hot plate. The liquid agar dispersion was poured into a 37mm petridish and cooled overnight at room temperature for testing 24 h later (± 2 h). Commercial food wrapping foil with 15µm thickness (Poylethylen, Aromata, Lidl) was tightened without air traps on top of the agar gel and fixed on the petridishes rim.
A 1mm long and 90µm diameter tungsten rod with a flat end was fixed by a Luer-connector in a high precision commercial 5DOF stereotactic frame (SASSU, pro-medTEC GmbH, Lübeck) [20] equipped with a force measuring load cell (±300mN, SS2 Sherborne Sensors, Hampshire, UK).
The frame reached a maximum insertion speed of up to 3mm/s. We determined by video analysis (see Fig. 2) the actual time spans from first contact of the probe with the foil/agar model to the ruptur ing of the foil for six different indentation speeds (0.25, 1, 2, and 3mm/s).

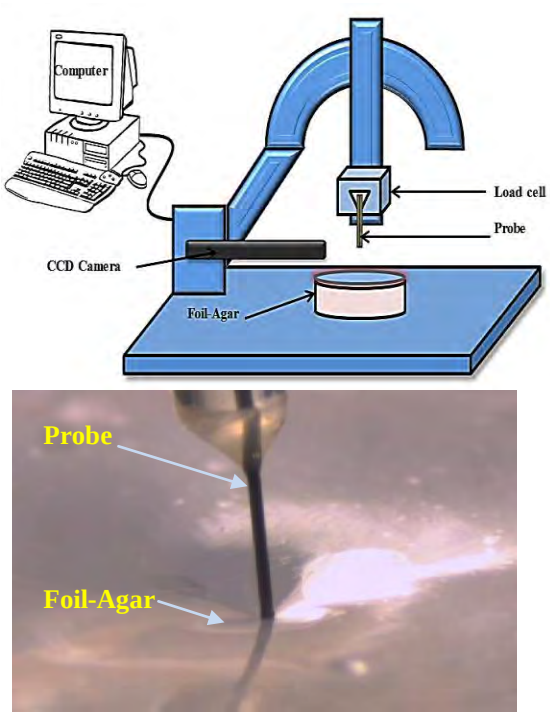

Figure 2: (top) Sketch of experimental setup to measure probe indentation into brain model; (bottom) single video frame from 0,25mm/s indentation of a 90µm tungsten rod into PE foil/1%agar substrate.

Load cell readouts during penetration are recorded as output voltage per time (data logger DI-718b USB, Dataq Instruments, Akron,OH). These values are then converted to forces with help of the documented the load cell sensitivity and the known SASSU parameters.

3. Results

3.1. FEM results

The simulation of the two-layer structure displayed the experimentally recognizable deformation and thus effects of dimpling, but was limited to an unruptured top layer.

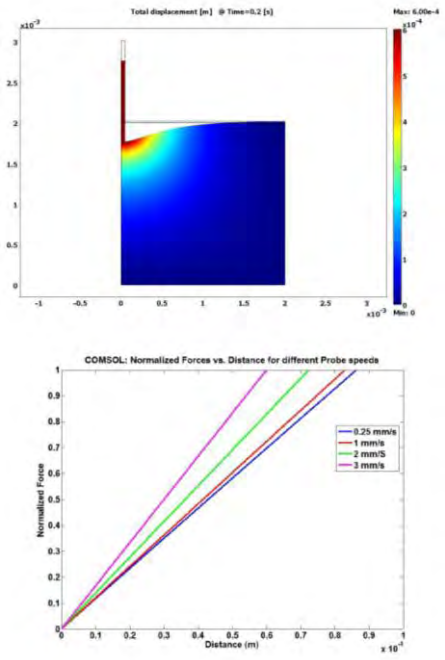

Figure 3: (top) Simulation of indenting a blunt tip into our layered model with 5mm/s speed; (bottom) Normalized force-distance plot for six different indentation speeds (0.25, 1, 2, and 3mm/s).

Consequently, we only display the spatial deformation of the indentation, caused by a displacement of the bulk agar under the top membrane (see Fig. 3 top). Displaying force vs. distance curves showed a quite characteristic linear increase in forces, until the van Mises stresses in the pial simulation exceeded the critical value, where the force relaxes in the experiment by breaking through the membrane (Fig. 5). To keep results comparable (absolut data not shown), we normalized the force-distance curves to the maximum force prior to pial rupture. When comparing the slopes of these curves, a clear dependency on the simulated penetration speed can be seen (Fig. 3 bottom).
Closer investigation of the possible location of rupture in the pial membrane during increasing loads shows excessive peaking of van Mises stress at the edges of the indenter (Fig. 4).

3.2. Foil/Agar indentation

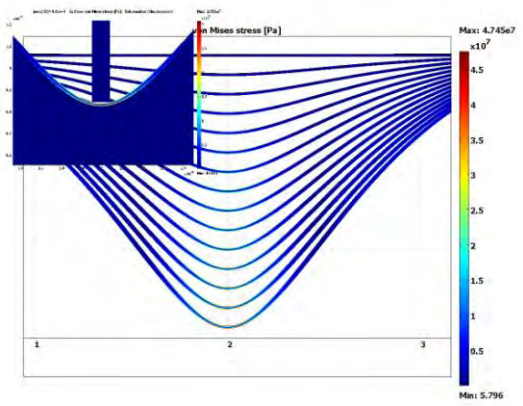

Figure 4: (insert) Simulation of a blunt indenter into a layered model; (graph) Overlay of consecutive time steps of indentation, indicating an increasing van Mises stress at the probes front edge.

Indentation of a tungsten rod into the foil/agar layer showed qualitatively a dimpling effect comparable to that of a microprobe through a rat's pia. However, when the penetration force with the former reached 30mN, forces with the latter stayed below 10mN (for a 50µm tungsten rod) [21].
When force-distance curves on foil/agar are displayed, they show an almost linear increase in force after first contact, which corresponds nicely to the simulated curve shapes. Even the speed dependency of the curves are maintained, when normalizing the measured forces to the maximum (penetration) force (see Fig. 5).

The elastic modulus of 1% Agar was calculated with the following shear modulus formula

$$E = 2\,G\,(1+\nu)$$

with G beeing the shear modulus (4.667×10^3 Pa), ν the Poisson's ratio and E the elastic modulus [22].

Since the agar material is considered a viscoelastic material it's Poisson's ratio was assumed to be 0.5 [23]. Consequently elasticity of 1% Agar gel lies around 15kPa, which compares reasonably with results from living rat brain (6 - 20kPa) [25].

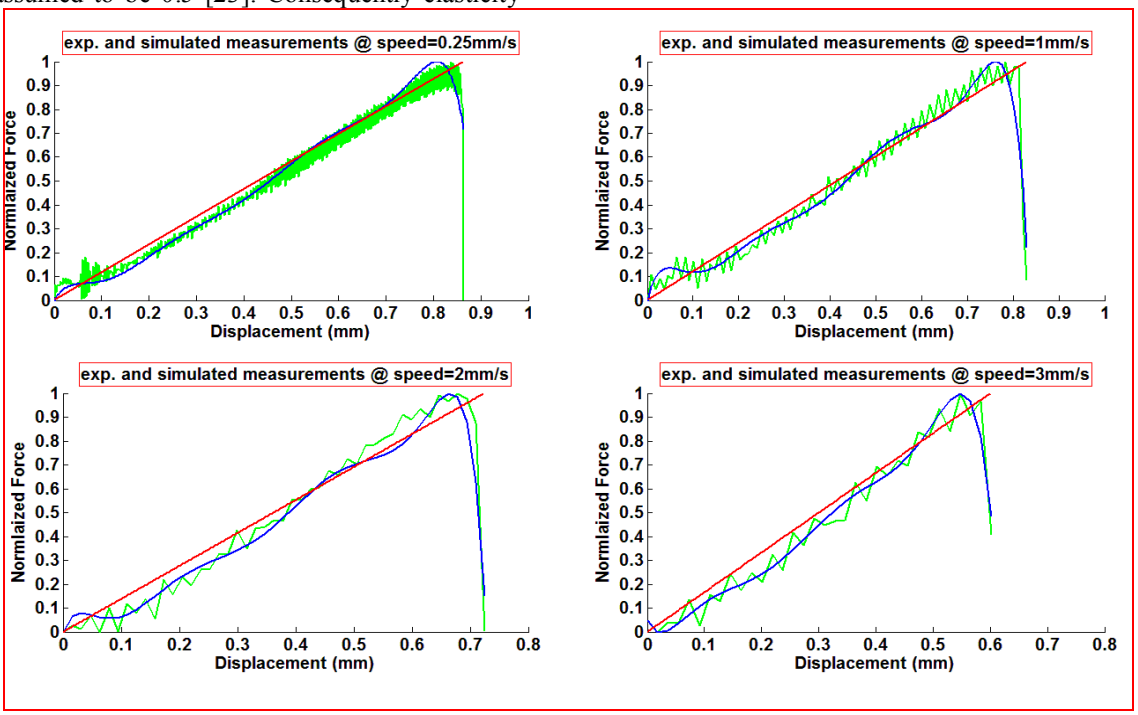

Figure 5: Force-distance curves for several indentation speeds. (green): experimental data, (blue): polynomial fit of experimental data and (red): FEM simulation result.

4. Discussion

Main motivation for this study was to provide the methodological means to evaluate new probe designs and implantation methods by reasonable models without the need to sacrifice animals. Even though the physical simulated elasticity of 1% agar falls in the same range as cortical rat brain does, agar itself is not suitable to solely model the real tissue. This is mainly due to the lack of a tough surface membrane on agar, as can be found in the hard to remove pia mater of the animal's brain.

Consequently some surface layer has to be introduced, which at least somewhat resembles the elastic properties of the pial membrane. With the use of PE-food wrapping foil on top of agar, we are able to reproduce the recorded dimpling of the penetrated tissue and such are closer to the real situation. Still, even this model has its shortcomings, mainly since the PE foil does not completely copy the pia, which makes it seemingly harder to penetrate and thus needs higher implantation forces, not to be reached by silicon probes!

However, a FEM simulation may very well be able to provide desired model. Our two layer indenter model at least provided results for different indentation speeds we tried, which very well match the implantation behaviour, except (due to numerical reasons) the rupturing itself.

At least the FEM simulation gave by hints as to where the rupturing will occur, according to its van Mises stress distribution. This approach will in the future enable us optimize micromachined probe shapes to enable elegant implantation without forced insertion. Up til then we do suggest the use of high speeds for implantation through the pia over slow and careful implantation.

5. Acknowledgements

Part of this work was supported by the BMBF-grant 13N9190 “BiCIRTS”.

6. Literatur

1. Hosford, W.F., Mechanical behavior of Materials,. 2005 Cambridge University Press.
2. Chapin, J.K., et al., Real-time control of a robot arm using simultaneously recorded neurons in the motor cortex. Nature Neuroscience, 1999. 2: p. 664-670.
3. Nicolelis, M.A.L., Advances in neural population coding. Progress in Brain Research. Vol. 130. 2001, Amsterdam: Elsevier.
4. Nicolelis, M.A.L. and J.K. Chapin, Controlling robots with the mind, in Scientific American. 2002. p. 24-31.
5. Schwartz, A.B., Cortical neural prostheses. Ann. Rev. Neurosci., 2004. 27: p. 487-507.
6. Hochberg, L.R., et al., Neuronal ensemble control of prosthetic devices by a human with tetraplegia. Nature 2006. 442: p. 164-171.
7. Polikov, V.S., P.A. Tresco, and W.M. Reichert, Response of brain tissue to chronically implanted neural electrodes J Neurosci Methods, 2005. 148(1): p. 1-18.
8. Szarowski, D.H., et al., Brain responses to micro-machined silicon devices. Brain Res 2003. 983(1-2): p. 23-35.
9. Silver, J. and J.H. Miller, Regeneration beyond the glial scar. Nat Rev Neurosci, 2004. 5(2): p. 146-156.
10. Leach, J., A.H. Achyuta, and S.K. Murthy, Bridging the divide between neuroprosthetic design, tissue engineering and neurobiology. Front. Neuroeng., 2010.
11. Biran, R., D.C. Martin, and P.A. Tresco, The brain tissue response to implanted silicon microelectrode arrays is increased when the device is tethered to the skull. Journal of Biomedical Materials Research Part A, 2007. 82(1): p. 169-178.
12. Turner, J., et al., Cerebral astrocyte response to micromachined silicon implants. EXPERIMENTAL NEUROLOGY, 1999. 156(1): p. 33-49.
13. Rousche, P.J., et al., Flexible Polyimide-based intracortical electrode arrays with bioactive capability. IEEE Trans Biomed Eng, 2001. 48: p. 361-371.
14. Knoll, W., et al., Tailoring of surfaces with ultrathin layers for controlled binding of biopolymers and adhesion and guidance of cells. Israel Journal of Chemistry, 1996. 36: p. 357-369.
15. Purcell, E.K., et al., In vivo evaluation of a neural stem cell-seeded prosthesis. J Neural Eng, 2009. 6(2): p. 10.
16. Richter, A., et al. Applying controlled sheer stress on cell covered microprobes to simulate
brain insertion. in submitted to BMT 2010. 2010. Rostock: de Gruyter.
17. Rousche, P.J. and R.A. Normann, A method for pneumatically inserting an array of penetrating electrodes into cortical tissue. Ann. Biomed. Eng., 1992. 20: p. 413-422.
18. COMSOL3.5a material library. 2009.
19. Kim, G.-W., et al., Determination of the Viscoelastic Properties of Agar/Agar-Gelatin Gels Based on Finite Element Method Optimization. Food Sci. Technol. Res., 2008. 14(6): p. 525-532.
20. Ramrath, L., et al., Computer- and robot-assisted stereotaxy for high precision small animal brain exploration. Biomedizinische Technik / Biomedical Engineering, 2009. 54: p. 8-13.
21. Jensen, W., K. Yoshida, and U.G. Hofmann. In vivo implant mechanics of single-shaft microelectrodes in peripheral nervous tissue. in 3rd Int'l Conference on Neural Engineering. 2007. Hawaii, USA: IEEE.
22. Fung, Y.C., Foundations of Solid Mechanics. 1965, New York, NY: Prentice Hall.
23. Radmacher, M., M. Fritz, and P.K. Hansma, Imaging soft samples with the atomic force microscope: gelatin in water and propanol. Biophys. J., 1995. 69(July): p. 264-270.
24. Ross, K.A. and M.G. Scanlon, Analysis of the elastic modulus of agar gel by indentation. J Texture Studies, 1999. 30: p. 17-27.
25. Knopp, U., et al. Compression of the cerebral cortex during corticotomy: A study of dimpling in rats. in 55. Ann' Jahrestagung der Deutschen Gesellschaft für Neurochirurgie. 2004. Köln: gms German Medical Sciences.